A Comparison of Two Ways to Reducing the Mutual Coupling of Chipless RFID Tag Scatterers

Milan Svanda, Jan Machac, *Senior Member, IEEE,* Milan Polivka, *Member, IEEE,* Jaroslav Havlicek

***Abstract*—This paper presents two ways to reduce the mutual coupling between the resonators of the RFID chipless tags. This reduction significantly improves the uniformity of the RCS response of the tag over the operational frequency range from 2 to 4 GHz. The first modification to the tag layout is based on an inter-element rearrangement of the array elements. The second layout modification is based on narrowing the strip width and tapering the longitudinal dipole arms toward the open end. Significantly improved homogeneity of the RCS response in comparison with the original array of folded dipole scatterers was confirmed by simulation and by measurements of 20-bit chipless RFID transponders. The second modification further improves the frequency resolution, which may consequently provide higher encoding capacity in a unit area, but at the expense of a decreased RCS response.**

***Index Terms*—Chipless radiofrequency identification, radar cross section, scatterer.**

I. Introduction

RFID technology is wide spread in a number of areas today such as identification of articles in warehouses, presence systems in buildings, parking systems, check-in, logistic, etc. [1]. In several last years, researchers deal with development of RFID transponders for special applications, among that they can be counted identification of objects in losses environment such as metallic or liquid materials [2, 3] and human body [4, 5]. Next sensing of electrical or non-electrical quantities by means of connection of some sensorial function or external sensors with the RFID transponder is very topic trend now; [6, 7]. However for all from the above mentioned areas the inherence of a semiconductor chip on the transponder with the complex input impedance [8] is some disadvantage of this technology, which can lead to higher manufacturing complexity and consequently to the cost price increasing.

On the contrary the chipless RFID technology can offer a transponder structure that is cheaper than currently used tags with chips. Several important issues need to be solved in the design of uniplanar chipless tags based on a specific spectral signature response. The most fundamental issue is the response stability and the robustness of the radar cross section (RCS). The attainable surface density of the stored information (in bits per unit area) is another significant issue, as optical barcodes are currently more satisfactory. Recent developments in the field of fully-printable chipless RFID transponders is summarized e.g. in [9], [10].

Several configurations of printed one bit scatterers in microwave bands (e.g. 2 – 6 GHz) have been proposed, e.g. dipole strips [11], split ring resonators (SRR) and C-shaped folded dipoles [12-14]. Unfortunately a trade-off has to be found between the quality factor or the bandwidth, the RCS response, determined by the electrical size and the compactness of the array of scatterers. The C-shaped folded dipole [15], [14] which provides 44 MHz half-power bandwidth, a 65 quality factor, and a -29.84 dBsm RCS response at resonance frequency, is a promising structure. These scatterers were used in [12], [14] to form a 20-bit chipless rfid tag 25 × 70 mm in size, which operates in the 2 – 4 GHz frequency band. The RCS response contained 20 resonant peaks that differ in magnitude by up to 10 dB, and the peak-to-valley level changes between 1 dB and more than 10 dB. These parameters indicate significant non-uniformity of the RCS response of these tags, which limits the identification reliability of the transponder.

This paper proposes two modifications to the geometrical layout of the scatterer, with the aim of reducing the mutual coupling between the resonators. This significantly improves the uniformity of the RCS response of the tag. The second modification further improves the frequency resolution (increases Q), which may provide higher encoding capacity in unit area. It should be noted that this second improvement is at the expense of a decreased RCS response of the proposed transponder.

II. C-Shaped Dipole Chipless RFID Tag

The geometry of the uniplanar strip scatterers used here is based on the C-shaped folded dipole presented by Vena et al. in [12]; see Figs. 1a and 2a. In order to make a correct comparison between the performance of the original Vena chipless RFID tags and both of our newly-proposed chipless RFID tags, we designed and simulated all transponders on a low-permittivity Rogers RO 4003 woven-glass laminate with relative permittivity $\varepsilon_r = 3.38$, and loss tangent $\tan \delta = 0.002$, with thickness of 0.2 mm, which provides a lower dielectric loss and a higher-quality coefficient of the scatterers than those manufactured onto the 0.8 mm FR-4 substrate used in [12], [14].

This work was supported by Czech Science Foundation under projects GA15-08803S, and GA13-09086S.
The authors are with the Department of Electromagnetic Field, Czech Technical University in Prague, Technicka 2, 166 27 Prague, Czech Republic (e-mail of the corresponding author: svandmil@fel.cvut.cz).
Digital Object Identifier inserted by IEEE.

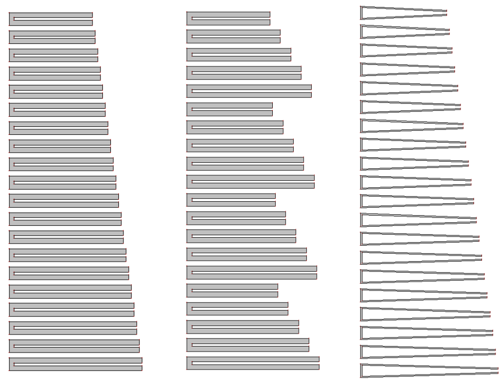

(a) (b) (c)

Fig. 1. Original (a), element rearranged (b), and tapered (c) configurations of the layouts of 20-bit chipless tags composed of an array of C-shaped strip scatterers representing the bit word '11111111111111111111'.

Chipless RFID transponders composed of 20 C-shaped strip scatterers representing the bit words '11111111111111111111' and '11111011111111011111' were simulated by the IE3D Methods of Moment software and were measured; see Figs. 1a and 2a. The external dimensions of the largest element are 25.5 × 2.5 mm, while the dimensions of the smallest element are 16 × 2.5 mm. The strip width is 1 mm and the gap size is 0.5 mm. The distance between each two neighboring elements is 1 mm.

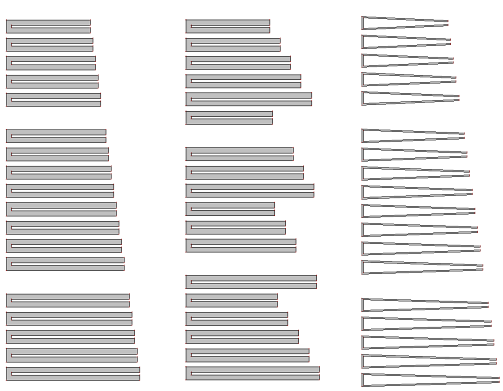

(a) (b) (c)

Fig. 2. Original (a), element rearranged (b), and tapered (c) configurations of the layouts of a 20-bit chipless tag, composed of an array of C-shaped strip scatterers representing the bit word '11111011111111011111'.

III. Reducing the Mutual Coupling

The investigated 20-bit C-shaped folded dipole transponder has promising properties for the coded '11111111111111111111' bit word; see Fig. 3. However, when several "0" bits are coded the uniformity of the tag RCS response is significantly disrupted. This can lead to unreliable identification of the whole tag. This phenomenon is caused by mutual coupling of neighboring scatterers, which results in frequency offset and also amplitude offset of the resonance peaks in the vicinity of the "0" bit resonator. In order to eliminate this phenomenon, we have proposed two ways to reduce the mutual coupling.

The first way involves modifying the inter-element arrangement of the scatterers in the tag configuration; [15]. The resonators are subdivided into four sub-arrays. In these subarrays, each resonator is now next to the originally fourth-in-length resonator from it. Consequently, the original ascending order according to the resonator length '1 2 3 4 5 6 7 8 9 10 11 12 13 14 15 16 17 18 19 20' is modified to '1 5 9 13 17, 2 6 10 14 18, 3 7 11 15 19, 4 8 12 16 20'; see Fig. 1b. In the new arrangement, the resonators with neighboring resonance frequencies are located far away and their mutual coupling is substantially reduced.

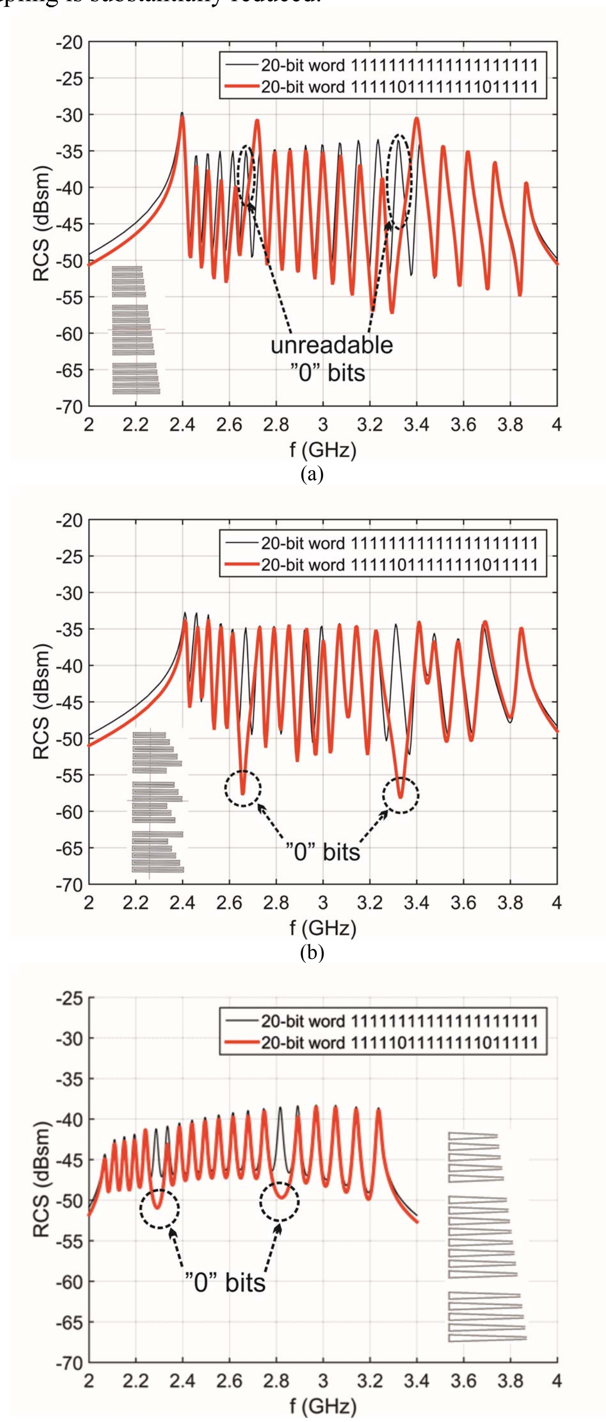

(c)

Fig. 3. Simulated RCS response of a 20-bit chipless tag composed of an array of C-shaped strip scatterers representing the bit words '11111111111111111111' and '11111011111111011111' in the original (a), element rearranged (b), and tapered (c) configurations.

The second way is based on modifying the geometry of the scatterers. This involves narrowing the strip width from the original 1 mm to 0.25 mm, and tapering the longitudinal dipole arms toward the open end of the scatterer [16]. This taper shape reduces the mutual coupling, since the directly neighboring arms are spatially separated. The drawback to this solution is that there is a lower RCS response, as the area of the scatterer is reduced.

The RCS responses of the 20-bit tags, simulated by Zeland IE3D Method of Moment software, are plotted in Fig. 3. We can observe a significantly smaller frequency shift and also better amplitude uniformity for both modifications presented here, in comparison with the original geometry. In addition, significant reduction of the frequency bandwidth is apparent for the tag with tapered scatterers.

IV. Measurements of Tag Performances

To verify the simulated results, we made a monostatic measurement of the RCS performance of tags in an anechoic chamber; see Fig. 4. The measurement was based on an evaluation of the reflection coefficient of a double ridge horn antenna DRH 20 [17], in front of which a scatterer was placed at a distance of 20 cm. The RCS response of the tag was calculated by the relation used in [14] that was modified so that it is applicable to the one-port case

$$\sigma^{tag} = \left(\frac{S_{11}^{tag} - S_{11}^{iso}}{S_{11}^{ref} - S_{11}^{iso}} \right)^2 \sigma^{ref} , \qquad (1)$$

where S_{11}^{tag} is the reflection coefficient measured with the scatterer. S_{11}^{ref} represents the reflection coefficient measured with a reference plate as the scatterer. S_{11}^{iso} is the reflection coefficient of the antenna itself measured without a scatterer, in order to eliminate the residual reflections from the experimental setup. σ^{tag} is the RCS of the measured tag, and σ^{ref} is the RCS of the reference scatterer, which is a rectangular metal plate $25 \times 70\ \mathrm{mm}^2$ in size and 0.3 mm in thickness. The analytical formula for its RCS is as follows:

$$\sigma^{ref} = 4\pi \frac{a^2 b^2}{\lambda^2} . \qquad (2)$$

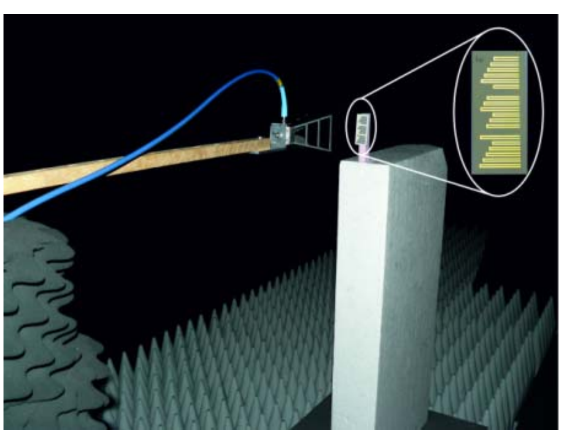

Fig. 4. Measurement setup using a monostatic measurement configuration with a detail of the element-rearranged 20-bit tag.

A comparison between the performance properties of the two modified geometries and the original geometry in a 20-bit arrangement is shown in Figs. 3 and 5, and is summarized in Table I. The measurements show that the two modifications presented here have a significantly smaller frequency shift and better amplitude uniformity than for the original geometry.

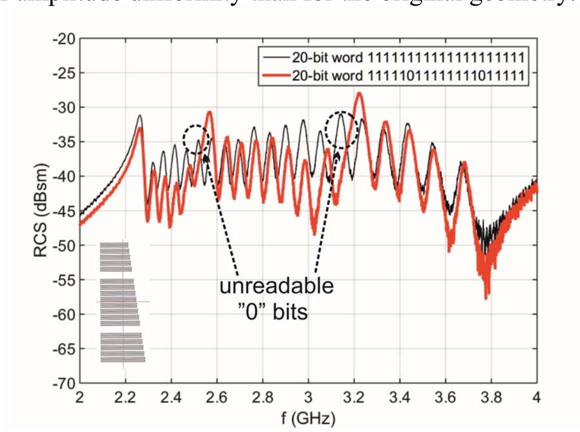

(a)

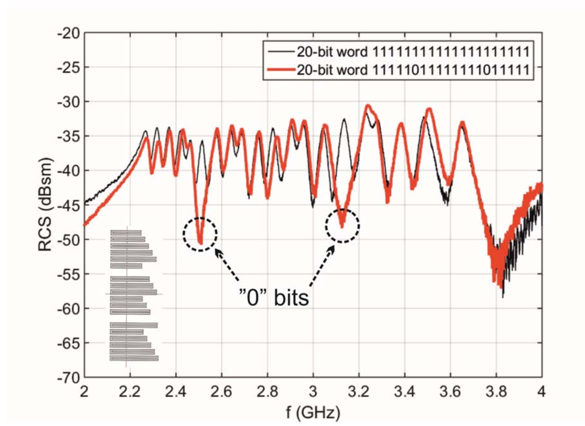

(b)

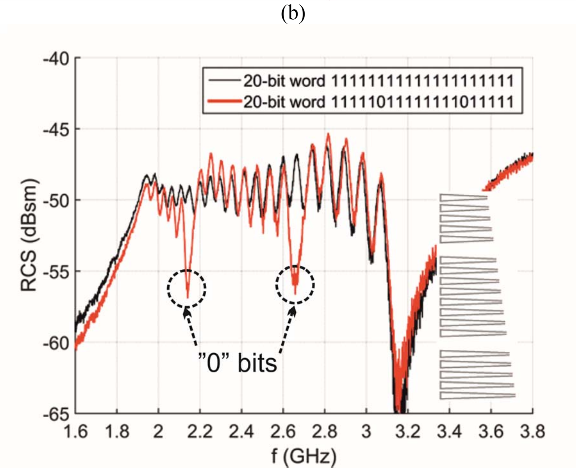

(c)

Fig. 5. Measured RCS response of a 20-bit chipless tag composed of an array of the C-shaped strip scatterers representing the bit words '11111111111111111111' and '11111011111111011111' in the original (a), element rearranged (b), and tapered (c) configurations.

In the case of the element rearranged tag, the difference between the highest resonance peak and the lowest resonance peak $\Delta\mathrm{RCS}_{\mathrm{MAX}}$ is just about 5 dB for both the simulated data and the measured data; see Figs. 3b and 5b. In the case of the tapered scatterers, the difference ΔRCS_{MAX} is likewise about 6 dB for the simulated data and 4 dB for the measured data, see Figs. 3c and 5c. This phenomenon represents a significant improvement of the RCS response uniformity in comparison with the original arrangement of the scatterers, where ΔRCS_{MAX} reaches about 10 dB for the simulated data and even more than 15 dB for the measured data.

In addition both modifications to the geometry presented here show significantly better frequency and amplitude stability in the case of "0" bit encoding; see Figs. 3 and 5. This is in contrast with the original arrangement, where the "0" bit is very difficult to recognize owing to mutual coupling of the neighboring scatterers, which results in frequency and amplitude offset of the resonance peaks in the vicinity of the "0" bit resonator.

The tapered scatterer tag provides a further benefit by reducing the frequency bandwidth. Its measured value is 60 MHz per bit. The lower RCS response level (-50 to -46 dBsm) is a disadvantage of this solution in comparison with the original geometry and the element rearranged geometry.

TABLE I
MEASURED PERFORMANCE PROPERTIES OF CHIPLESS RFID TAGS.

Tag configuration	Frequency band (GHz)	BW (GHz)	BW per bit (MHz/bit)	RCS_{MAX} (dBsm)	ΔRCS_{MAX} (dB)
Original	2.2 to 3.7	1.5	75	-42 to -27	15
Element rearranged	2.2 to 3.7	1.5	75	-35 to -30	5
Tapered	1.9 to 3.1	1.2	60	-50 to -46	4

BW – frequency bandwidth of the RCS
RCS_{MAX} – the highest level of peaks in the RCS response
ΔRCS_{MAX} – difference between the highest and the lowest resonance peak

V. CONCLUSION

Two modifications to the geometrical layout of a scatterer have been proposed and verified by simulation and by measurements of 20-bit tags coding two different bit words. The modified geometry reduces the mutual coupling between neighboring scatterers, and therefore significantly improves the uniformity of the chipless RFID tag RCS response.

A significant improvement in the RCS response amplitude uniformity and also in the frequency stability, when the "0" bits are encoded was confirmed for both of the proposed geometries. The tapered arms scatterers further improve the frequency resolution, which may consequently provide higher encoding capacity in a unit area, but at the expense of a decreased RCS response.

Thanks to their improved properties and their simple geometry, the tags presented here are good candidates for printed and low-cost chipless RFID applications.

REFERENCES

[1] K. Finkenzeller, "RFID Handbook: Fundamentals and Applications in Contactless Smart Cards and Identification", 2nd edition, John Wiley & Sons, 2005.

[2] M. Svanda and M. Polivka, "Horizontal Five-Arm Folded Dipole over Metal Screening Plane for UHF RFID of Dielectric Objects," *Microw. and Optical Technology Lett.*, vol. 52, issue 10, pp. 2291-2294, 2010.

[3] A. Ali Babar, at al., "Small and flexible metal mountable passive UHF RFID tag on high-dielectric polymer-ceramic composite substrate," *IEEE Antennas Wireless Propag. Lett.*, no. 11, pp. 1319-1322, 2012.

[4] M. Svanda and M. Polivka, "Matching Technique for an On-Body Low-Profile Coupled-Patches UHF RFID Tag and for Sensor Antennas", *IEEE Trans. on Antennas and Propag.*, vol. 63, No. 5, pp. 2295-2301, 2015.

[5] M. Svanda, M. Polivka, and P. Hudec, "Novel Low-Profile Foam Dielectric Over the Shoulder Antenna Based on Coupled Patches Technique", *Microw. and Optical Technology Lett.*, vol. 55, issue 3, pp. 593-597, 2013.

[6] C. Occhiuzzi, S. Caizzone, and G. Marrocco, "Passive UHF RFID Antennas for Sensing Applications: Principles, Methods and Classifications", *IEEE Antennas and Propag. Mag.*, vol. 55, issue 6, pp. 14-34, 2013.

[7] J. Kracek, M. Svanda, M. Mazanek, and J. Machac, "Implantable Semi-Active UHF RFID Tag with Inductive Wireless Power Transfer," *IEEE Antennas and Wireless Propag. Lett.*, 2016, in press.

[8] M. Polivka, A. Holub, M. Vyhnalik, and M. Svanda, "Impedance Properties and Radiation Efficiency of Electrically Small Double and Triple Split-Ring Antennas for UHF RFID Applications," *IEEE Antennas and Wireless Propag. Lett.*, vol. 12, pp. 221-224, 2013.

[9] S. Preradovic and N. C. Karmakar, "Chipless RFID: Bar Code of the Future," *IEEE Microwave Magazine*, vol. 11, no. 7, pp. 87-97, Dec. 2010.

[10] S. Preradovic and N. C. Karmakar, "Advanced Radio Frequency Identification Design and Applications, Fully Printable Chipless RFID, " Tag (chapter 7), InTech, 2011.

[11] I. Jalaly and I. D. Robertson, "RF Barcodes Using Multiple Frequency Bands, " IEEE MTT-S Int. Dig., Long Beach, CA, Jun. 2005, pp. 139-141.

[12] A. Vena, E. Perret, and S. Tedjini, "Chipless RFID Tag Using Hybrid Coding Technique, " *IEEE Trans. Microw. Theory Tech.*, vol. 59, no. 12, pp. 3356-3364, Dec. 2011.

[13] A. Vena, E. Perret, and S. Tedjini, "Design of Compact and Auto-Compensated Single-Layer Chipless RFID Tag," *IEEE Trans. on Microw. Theory Techn.*, vol. 60, no. 9, pp. 2913-2924, Sept. 2012.

[14] A. Vena, E. Perret, and S. Tedjini, "A Fully Printable Chipless RFID Tag With Detuning Correction Technique", *IEEE Microw. and Wireless Component Lett.*, vol. 22, no. 4, pp. 209-211, Apr 2012.

[15] M. Polivka, J. Havlicek, M. Svanda, and J. Machac, "Improvement of RCS Response of U-Shaped Strip-Based Chipless RFID Tags," Proc. of European Microw. Conf. (EuMC), 2015 45th, Paris, France, pp. 107-110, 6-11 Sep. 2015.

[16] M. Polivka and J. Machac, "Improvement of Backscatter Properties of C-Shaped Dipole Scatterer for Chipless RFID," Proc. of Asia Pacific Microw. Conf. (APMC), 2014, pp. 962-964, 4-7 Nov. 2014.

[17] Model DRH20 - Double ridge waveguide horn. RFspin s.r.o., 6.11.2015. [Online]. Available at http://www.rfspin.cz/en/antennas/drh20.php.